

Elsevier Editorial System(tm) for Journal of Process Control

Manuscript Draft

Manuscript Number:

Title: Control of fuel-cell power output

Article Type: Research Paper

Section/Category:

Keywords: Fuel cell; DC/DC converter; electric motor

Corresponding Author: Federico Zenith, MSc

Corresponding Author's Institution: Norwegian University of Science and Technology

First Author: Federico Zenith, MSc

Order of Authors: Federico Zenith, MSc; Sigurd Skogestad, PhD

Manuscript Region of Origin:

Abstract: A simplified dynamic model for fuel cells is developed, based on the concept of instantaneous characteristic. This is used to derive a theorem that indicates the conditions under which the power output of fuel cells can, in theory, be perfectly controlled. A fuel cell connected to a DC/DC converter is simulated numerically using a control system based on switching rules. This algorithm is then inserted in a cascade control loop to control the torque output of a DC electric motor with a PI controller in the external loop.

# Control of fuel-cell power output

Federico Zenith<sup>a</sup>, Sigurd Skogestad<sup>a,\*</sup>

<sup>a</sup>*Department of Chemical Engineering, Norwegian University of Science and Technology, Sem Sælands veg 4, 7491 Trondheim, Norway*

---

## Abstract

A simplified dynamic model for fuel cells is developed, based on the concept of instantaneous characteristic. This is used to derive a theorem that indicates the conditions under which the power output of fuel cells can, in theory, be perfectly controlled. A fuel cell connected to a DC/DC converter is simulated numerically using a control system based on switching rules. This algorithm is then inserted in a cascade control loop to control the torque output of a DC electric motor with a PI controller in the external loop.

*Key words:* Fuel cell, DC/DC converter, electric motor

---

## 1 Introduction

Fuel cells are devices that convert chemical energy (often in the form of hydrogen) into electricity, without passing through a combustion stage. While few fuel-cell-based devices are currently available to consumers, they have the potential to be used, in different layouts and types, to provide electric power to utilities as diverse as cars, laptop computers, mobile phones, or even to the electric grid as a power station. Research in all of these areas is extensive. However, the dynamics of fuel cells has received comparatively less attention; control of fuel cells has received even less attention.

The focus of this paper is on controlling the power output delivered to an electric motor through a DC/DC converter. This is currently the least studied aspect of control of fuel cells, but also one of its most important issues. In

---

\* Corresponding author. Tel. +47 73 59 41 54, Fax +47 73 59 40 80.

*Email addresses:* [zenith@chemeng.ntnu.no](mailto:zenith@chemeng.ntnu.no) (Federico Zenith),  
[skoge@chemeng.ntnu.no](mailto:skoge@chemeng.ntnu.no) (Sigurd Skogestad).

<b>Nomenclature</b>		
$C$	Capacitance	[F]
$D$	Duty ratio	[-]
$E$	Reversible potential	[V]
$F$	Force	[N]
$i$	Current density	[A m <sup>-2</sup> ]
$I$	Current	[A]
$L$	Inductance	[H]
$P$	Power	[W]
$R$	Resistance	[Ω]
$T$	Torque	[N m]
$v$	Velocity	[m s <sup>-1</sup> ]
$V$	Voltage	[V]
$Z$	Impedance	[Ω]
$\eta$	Overvoltage	[V]
$\Phi$	Magnetic field	[Wb]
$\omega$	Angular velocity	[rad s <sup>-1</sup> ]

addition, control algorithms for flows, temperature and other variables may be needed, but these are outside the scope of the paper.

## 1.1 Literature Review

### 1.1.1 Dynamics

Most dynamic models of fuel cells, such as for example in Amphlett et al. [1], normally consider current to be the system's input. While this is legitimate in a dynamic model, it must be remembered that current is not a directly manipulable input variable: it is rather the control objective than the means of control. Therefore, many models found in the literature will have to be adjusted to use manipulable inputs before they can be useful in a process-control setting. A proper means of control has to be clearly identified.

The model produced by Amphlett et al. [1] is essentially a thermal model with a basic, empirical modelling of the overvoltage effects. Cell current is considered a system input, and the catalytic overvoltage is assumed to vary instantly as a function of temperature, oxygen concentration and current. The

model predicts well the behaviour of the stack in a time scale of minutes, but, since it does not treat the overvoltage as a state, it might be less accurate in the scale of seconds and lower.

Ceraolo et al. [2] developed a dynamic model of a PEM fuel cell that included the dynamic development of the catalytic overvoltage. Whereas they did not apply their results to control, they produced a model that could easily be modified for control applications; they also included a model for multicomponent diffusion on the cathode side, based on Stefan-Maxwell equations.

Pathapati et al. [3] produced a model that calculated the overvoltage as in Amphlett et al. [1], integrating the catalytic overvoltage and non-steady-state gas flow analysis.

### 1.1.2 Control

Two similar US patents have been granted to Lorenz et al. [4] and Mufford et al. [5], both concerning methods to control the power output of a fuel cell. Both these methods use air inflow as the input variable. While this variable can indeed be set by manipulating the air-compressor speed, there are various reasons why this choice of input variable is not successful. First of all, only the fuel cells *per se* are considered: vital information is lost about the utility that will draw power from the cell. Also, while it could seem intuitive that a fuel cell will produce more power the more oxidant it is fed, this neglects a series of phenomena such as the mass-transport limit, the strong nonlinear effects of oxygen partial pressure in the cathode kinetics, the diffusion of oxygen through the cathode and the accumulation of oxygen in the cathode manifold.

In the PhD thesis by Jay Pukrushpan [6] there is a lot about control of fuel cell systems, with focus on air-flow control and a large section about control and modelling of natural-gas fuel processors. Notwithstanding the high quality of the work, Pukrushpan has seemingly misquoted another author, Lino Guzzella [7], claiming that the time constants of electrochemical phenomena in fuel cells are in the order of magnitude of  $10^{-19}$  seconds (Guzzella himself claimed  $10^{-9}$  seconds). Pukrushpan did therefore not elaborate further on the electrochemical transient, whereas other authors have found that the time constants for the electrochemical transients are actually much higher [2,3,8,9].

Johansen investigated, in his MSc thesis [10], the possibility of using reactant feed rate as an input in a control loop. As shown in figure 1, when the feed rate<sup>1</sup> was shut down, the fuel cell continued to produce power at an almost undisturbed rate, but dropped later, after about one minute. On the other

---

<sup>1</sup> Johansen modified the hydrogen feed rate, but his conclusion is specular for oxygen on the cathodic side.

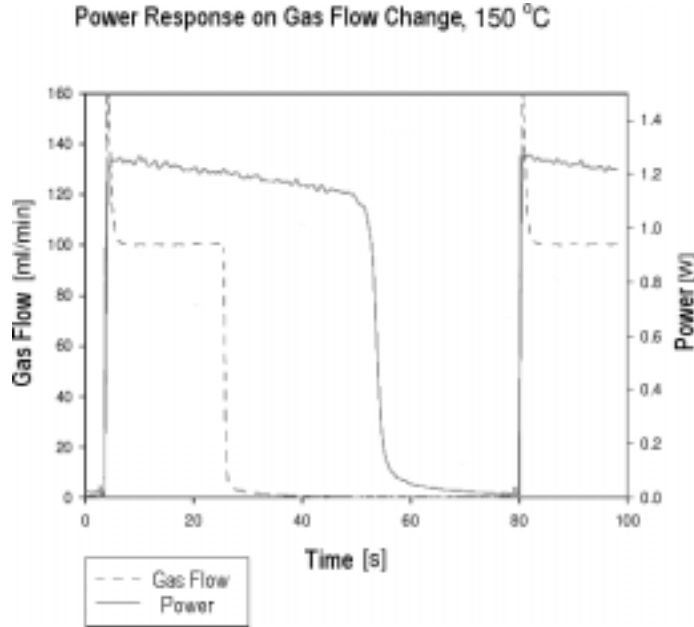


Fig. 1. Experimental data showing the relationship between reactant feed rate to a fuel cell and the cell's power output (from Johansen [10]).

hand, as soon as the reactant feed was reopened, the power output immediately reattained the previous values. This indicates that there is a dead time in which reactants in the manifolds must be consumed before the effect of reduced partial pressure can be apparent; the actual extent of this delay will depend, among other things, on the sizing of the manifolds and on the rate of consumption of reactants. This effect, which is the same one encountered at the mass-transport limit when operating a fuel cell in normal conditions, is known to be nonlinear with reactant concentration, and its occurrence roughly corresponds with the depletion of one of the reactants. It must also be remarked that these effects are often not known precisely, as the cell's behaviour depends on many variables such as temperature, humidification, wear, and others.

Johansen's findings indicate that the feed rate of reactants, in the specific case of the two patents [4,5] oxygen, is a poor system input for a control layout. While it *can* be possible to control a fuel cell in such a way, the large delays and strong nonlinearities associated with the effect of the input on the system will eventually limit the system's performance in reference tracking and disturbance rejection. Furthermore, such a system would be an energetically inefficient *control through reactant starvation*.

Golbert and Lewin [11] studied the application of model-predictive control (MPC) to fuel cells. They claimed that a sign inversion in the static gain between power output and current barred the possibility of using a fixed-gain controller with integral action, since it could not have been stabilised on such a process. They proceeded therefore to synthesise an MPC controller. Through-

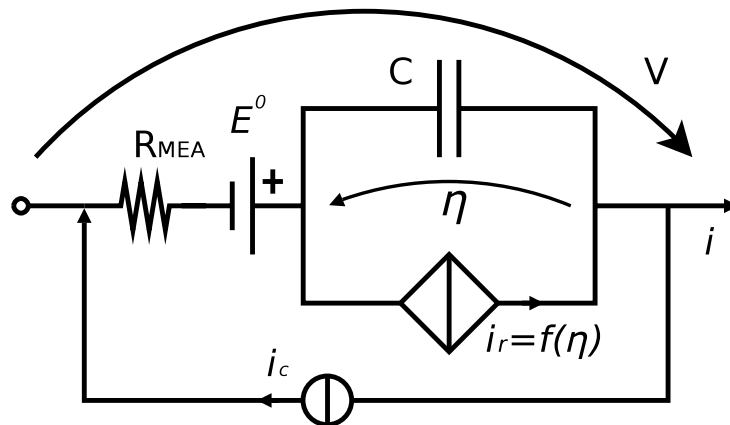


Fig. 2. A simplified model of a fuel cell, with only one electrode.

out the paper, Golbert and Lewin assume that current is a manipulable input, and use it to control the power output. However, Jay Benziger pointed out that it is not possible to use current (or voltage, which Golbert and Lewin’s model also allows) as an input: he suggested the resistance of the external circuit as the variable one should rather use [12].

One of the currently only two articles about fuel cells in the Journal of Process Control was written by Caux et al. [13]. They consider a system comprising a fuel cell, a compressor, valves, two DC/DC converters (a booster and a buck-boost converter). The analysis of the complete system is a step forward from the studies where the fuel cell had been seen as a separate entity from the rest of the process, but the fuel cell model itself is the same as from Amphlett et al. [1], and is therefore not treating overvoltage as a state; voltage variations will therefore be caused, directly, only by variations in temperature, current or oxygen concentration.

## 2 The Dynamic Model

In order to control fuel cells, it is useful to first present a dynamic model, in order to better understand the system. A previously developed model [9] will be summarised in this section.

Figure 2 shows how we can model a fuel cell to simulate its dynamic properties related to the electrochemical transient; the main equations are given in table 1. This type of model is quite commonplace in electrochemistry, consisting of:

- a voltage generator,  $E^0$ ;
- a resistance,  $R_{MEA}$ ;

Cell voltage	$V = E^0 - \eta - R_{MEA} (i + i_c)$	(1)
Overvoltage differential equation	$\frac{d\eta}{dt} = \frac{i + i_c - i_r}{C}$	(2)
Butler-Volmer equation	$i_r = i_r(\eta, \dots)$	(3)
External load's characteristic	$f(i, V, t) = 0$	(4)

Table 1

Summary of the main equations used in the model.

- a single electrode (the cathode), with a capacitance  $C$  in parallel with a voltage-controlled current generator;
- a current generator,  $i_c$ , that forces a certain current through the cell, even when this is in an open-circuit configuration.

It must be kept in mind that the underlying hypothesis of this simplified model, i.e. neglecting the anode, will be invalid if the hydrogen flow will be contaminated with poisons such as CO; in such a case, both electrodes will have to be modelled.

The voltage generator  $E^0$  represents the reversible potential: it depends on temperature and concentration of reactants at the reaction sites, which in turn depends on the reaction current  $i_r$ . This dependence on reactant concentrations is however weak, except when some of these are close to zero. It can be calculated with thermodynamic data, and is often assumed constant at about 1.22 V.

The resistance in series with the generator,  $R_{MEA}$ , represents the resistance to proton conduction in the membrane, and any other resistances in series with it; its value depends mostly on temperature.

The capacitance  $C$  lumps together a series of phenomena, most importantly the charge double layer [3] but possibly some other ones, such as charged adsorbed species. It is assumed constant, but some sources indicate it might be somewhat variable [14].

The voltage-controlled current generator  $i_r(\eta)$  in parallel with the capacitance is represented, in much of the electrochemical literature, by a resistance. This can be misleading: this generator actually represents the Butler-Volmer [15] equation (3), that depends exponentially, not linearly, on the overvoltage  $\eta$ , and can depend strongly on many other factors, such as temperature, reactant concentration, presence of poisoning agents, etc.

The current generator,  $i_c$ , represents the crossover current, that lumps together a series of losses such as permeation of hydrogen or other reactants through the membrane, electronic conductivity of the membrane or similar ones. Its value is normally small, but has a significant effect: the overvoltage, especially

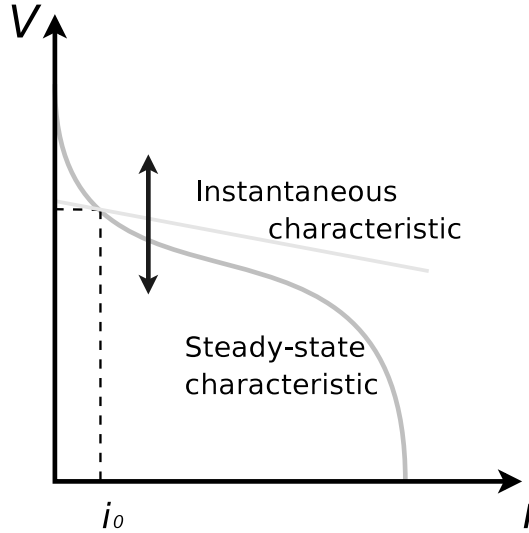


Fig. 3. The steady-state polarisation curve and the instantaneous characteristic on a  $V$ - $i$  plane. The instantaneous characteristic can move up or down according to the value of overvoltage  $\eta$ .

the cathode's, will increase rapidly at low values of current, and the presence of this small crossover current is what reduces the open-circuit voltage of the fuel cell from the theoretical value of the reversible potential. It is assumed to be constant.

### 3 Instantaneous characteristics

#### 3.1 Definition

In electrochemistry, the relationship between current density  $i$  and voltage  $V$  in a fuel cell is widely known as the polarisation curve. Polarisation curves represent the steady state, and do not contain information about the way the fuel cell will behave during transients. To include this information in the same plot, we define the *instantaneous characteristic* to be the locus of all points that can be reached instantaneously by the fuel cell in the  $V$ - $i$  plane. To define it, it is important to note which terms of the polarisation curve are going to change in a transient, and how so.

From a control point of view, the instantaneous characteristic comes from equation 1, where the terms  $V$  and  $i$  can change stepwise. The *state* of a system is defined as the set of variables needed to fully describe a dynamic system at a given time. In the case of the model in figure 2 and table 1, the voltage  $\eta$  across the capacitor is a state, since it represents the charge accumulated in



it, which evolves continuously in time according to equation 2. The reaction current  $i_r$ , which represents the consumption of reactants, is a continuous, strictly increasing function of  $\eta$ , according to the Butler-Volmer equation [15]:  $i_r$  is therefore continuous in time as  $\eta$  is. To any value of  $\eta$  corresponds one and one only value of  $i_r$ , so the state of the fuel cell may be described by  $i_r$  just as well as by  $\eta$ ; it is possible to express each one as a function of the other<sup>2</sup>. The reversible voltage  $E^0$  will also not have a discontinuity at step time, since it depends on  $i_r$ .

On the other hand, the current density  $i$  passing through the fuel cell is not a state, and it can change stepwise.

The equation for the cell voltage can be rewritten highlighting the dynamic and the algebraic parts as:

$$V(t, i) = \underbrace{E^0 - \eta}_{V_{dyn}(t)} - \underbrace{R_{MEA} \cdot (i + i_c)}_{V_{alg}(i)} \quad (5)$$

If we make a stepwise change in  $i$  at  $t = 0$ ,  $V_{dyn}$  will remain continuous, and it will have a single value at that time.  $V_{alg}$  will instead change instantaneously with  $i$ .

The instantaneous characteristic described by equation 5 can be seen as a line in the  $V$ - $i$  plane that will rise or descend according to the value of  $V_{dyn}(t)$ . It will be a straight line if  $R_{MEA}$  is constant, as shown in figure 3.

### 3.2 Application

We can now turn our attention to how specific transients develop. The values of voltage and current will be determined by the intersection between the instantaneous characteristics of the cell and the characteristic of the load. If the intersection point is not on the steady-state polarisation curve, the cell's instantaneous characteristic will rise or sink, until the operating point will be brought to the intersection between the load characteristic and the polarisation curve.

In general, the load might also be represented by an instantaneous characteristic, but for ease of treatment we will first consider only loads with a constant characteristic.

<sup>2</sup> On the other hand, the Butler-Volmer equation, expressing  $i_r = f(\eta)$ , cannot be solved explicitly for  $\eta$ , and requires an iterative loop. The Tafel equations are a very good approximation of  $\eta = f(i_r)$  at sufficiently large values of  $i_r$  [16].

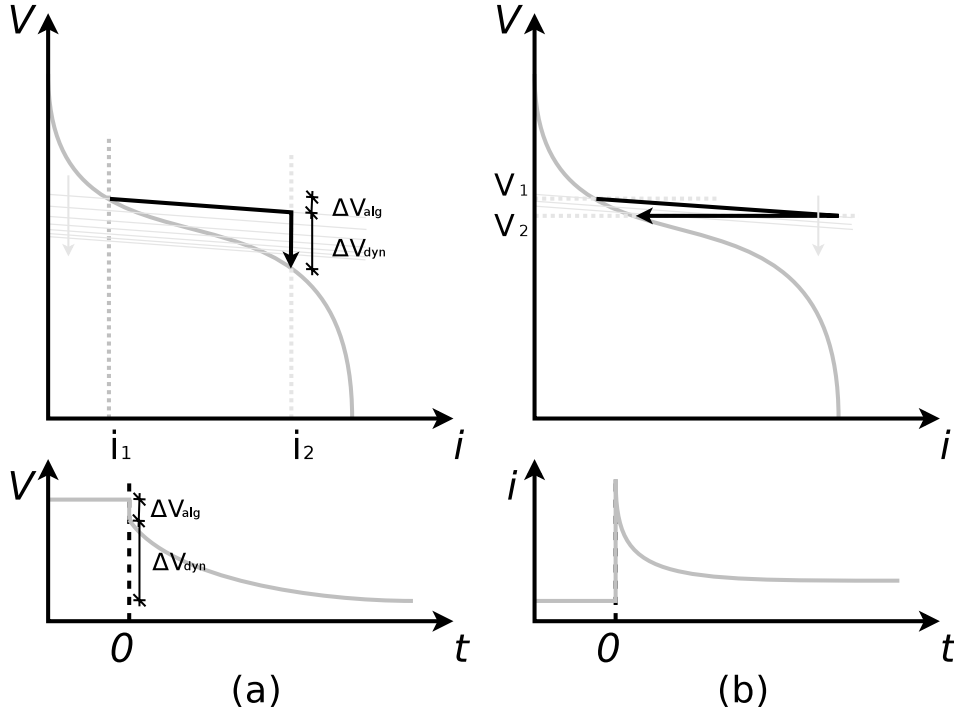


Fig. 4. Transients in the phase plane and in time when stepping (a) the cell current or (b) the cell voltage using a galvanostat or a potentiostat, respectively.

In figures 4 and 5, a few simple transients have been sketched. They all start from a steady-state point on the polarisation curve, and illustrate the path of the operating point to reach the new intersection between the load. All transients consist of two parts:

- (1) After the step has taken place, the operating point instantaneously moves to the intersection of the current instantaneous characteristic and the new load.
- (2) Remaining on the external load's characteristic, the operating point follows the movement of the instantaneous characteristic, until it settles on the intersection between the external load and the polarisation curve.

Whereas the plots in figure 4 assume the presence of a current or voltage generator, and therefore an external power supply, the ones in figure 5 assume loads that can be changed with little or no external power supply. A resistance step may be done with a simple switch or using a rheostat; a step in the gate voltage of a MOSFET<sup>3</sup> will require a voltage source, but this source will have to provide only a negligible amount of power. What is particularly interesting about rheostats or MOSFETs is that they can change their characteristic

<sup>3</sup> For a process engineer, MOSFETs can be thought as valves that allow more current through them when their gate voltage is increased. For a detailed treatise of MOSFETs, see e.g. Mohan et al. [17].

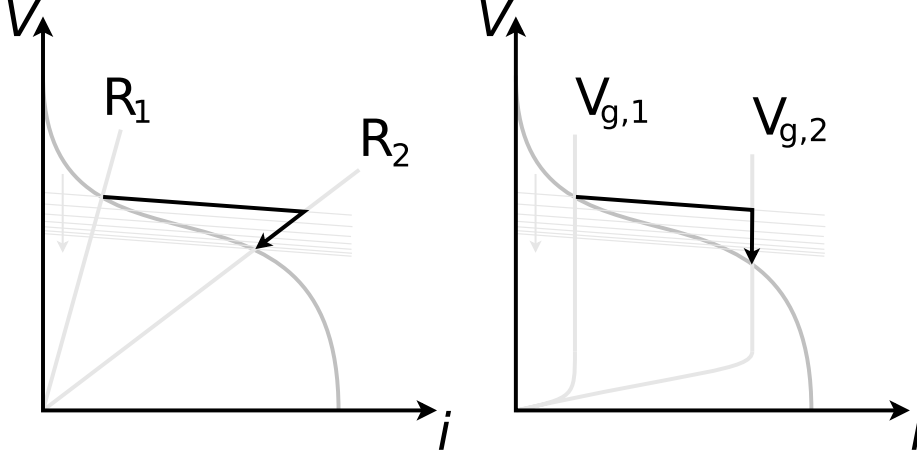


Fig. 5. Transients in the phase plane obtained by changing the external circuit’s characteristic, on the left with a resistance (stepping from  $R_1$  to  $R_2$ ) connected to the fuel cell, and on the right with a MOSFET whose gate voltage is stepped from  $V_{g,1}$  to  $V_{g,2}$ .

continuously with an input variable that can be directly manipulated.

### 3.3 Time constants of the electrochemical transient

The catalytic overvoltage varies according to the differential equation:

$$\frac{d\eta}{dt} = \frac{i + i_c - i_r}{C} = \frac{i - (i_r - i_c)}{C} \quad (6)$$

Since the level of the instantaneous characteristic is determined by the value of  $\eta$ , the right-hand side in equation 6 represents also the “speed” at which the instantaneous characteristics moves vertically on the plot. It is relatively easy to find  $i$  and  $i_r - i_c$  graphically: the circuit current,  $i$ , is at the intersection of the instantaneous characteristic with the external load; the reaction current minus the crossover current,  $i_r - i_c$ , is at the intersection of the instantaneous characteristic with the polarisation curve.

This claim can be demonstrated as follows: the polarisation curve represents the steady-state points, and the instantaneous-characteristic represents all points with the same  $\eta$  and  $i_r$ : their intersection is the steady-state with the same reaction current  $i_r$  of the transient operating point. Since at steady state, by equation 2,  $i_r - i_c = i$ , the projection of this intersection on the  $i$  axis is  $i_r - i_c$ , as illustrated in figure 6.

An interesting side effect is that some transients may have different time con-

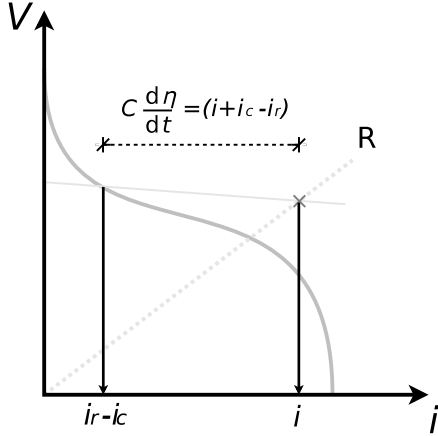


Fig. 6. The distance between the intersection points of the instantaneous characteristic with the external load and with the polarisation curve represents the driving force of the transient.

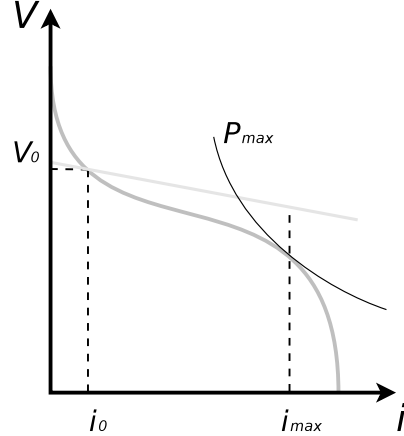


Fig. 7. At current  $i_{max}$ , where the steady-state power output is maximum, the instantaneous characteristic from point  $(i_0, V_0)$  has a higher voltage than the polarisation curve.

starts depending on how close to the polarisation curve their trajectory is. If a transient trajectory consists of points that are close to the polarisation curve<sup>4</sup>, the driving force of equation 6, i.e. the difference between  $i$  and  $i_r - i_c$ , is small, and the transient will be slower. This has been verified experimentally [9], and simulation indicates that times in the order of 10s are common to reach steady-state in open circuit. Settling times are typically in the range of 10 down to 0.1 s.

#### 4 Perfect Control of Fuel Cells

An important result can be obtained observing the instantaneous characteristics in the previous figures. We see clearly that they pass by the current corresponding to the maximum power output with an higher voltage than the polarisation curve, as exemplified in figure 7. It is an immediate observation that this means that we can, at least in theory, step the power output of the fuel cell even beyond the maximum nominal value. We shall now seek to properly formalise this finding.

We shall define  $P_{max}$  and  $i_{max}$  to be the power output and the current at the point, on the steady-state polarisation curve, where the power output from the cell is maximum.

<sup>4</sup> More rigorously: points lying on an instantaneous characteristic whose intersection with the polarisation curve is close, with distance being measured along the  $i$  axis.

**Theorem 4.1 (Perfect control of fuel cells)** *Given a fuel cell having its steady-state voltage expressed by  $V(i) = E^0 - \eta(i_r) - R_{MEA}(i)(i + i_c)$ , with overvoltage  $\eta(i_r)$  strictly increasing with  $i_r$ , and internal resistance  $R_{MEA}(i)$  continuous in  $i$ , it is always possible to instantaneously step the power output to any value between zero and its maximum steady-state value from any operating point, both transient and steady-state, lying on an instantaneous characteristic intersecting the polarisation curve at some  $i \in [0, i_{max}]$ .*

**Proof** Given any fixed  $i_0 \in [0, i_{max}]$ , we can identify the corresponding instantaneous characteristic  $V(i) = E^0 - \eta(i_0 + i_c) - R_{MEA}(i)(i + i_c)$ . Since  $\eta(i_r)$  is strictly increasing with  $i_r$ ,  $\eta(i_{max} + i_c) \geq \eta(i_0 + i_c)$ .

Subtracting the steady-state characteristic from the instantaneous one at  $i = i_{max}$ , we obtain  $-\eta(i_0 + i_c) + \eta(i_{max} + i_c) \geq 0$ , meaning that the instantaneous characteristic will have a higher voltage at  $i = i_{max}$ , and thereby a larger power output.

Power along the instantaneous characteristic varies continuously, according to the formula  $P(i) = V(i)i$ , because  $R_{MEA}(i)$  is also assumed continuous. It is trivial that power output can be set to zero by setting  $i = 0$ . For the intermediate-value property,  $\exists i : P(i) = P, \forall P \in [0, P_{max}]$ .  $\square$

This theorem guarantees, therefore, that there is a way to change instantaneously to any value of power output in the complete power range of the fuel cell, from zero to maximum, under very general conditions. This means there is no inherent limitation to how fast control we can achieve, even though practical issues such as measurement time and computation time will eventually pose a limit.

This has also other implications: if incorrectly controlled, a fuel cell might exhibit large spikes in power output, which may damage equipment connected to it. This might be especially important in microelectronics appliances.

#### 4.1 *Implicit Limitations*

Theorem 4.1 delivers an important result, but makes some implicit assumptions. The assumption about the form of the function describing the polarisation curve is especially important, since the curve is expected to be only a function of the circuit and reaction currents: other factors such as temperature, catalyst poisoning, reactant concentration are left out. Therefore, *the theorem is valid only in the context of a certain set of states* that define the polarisation curve: we are only guaranteed that we can instantly reach the maximum power output for those conditions of temperature, composition, etc., which may be less than the nominal power output that the fuel cell is supposed to deliver

in design conditions. In such a case, other control variables may be used to modify these states, and might pose some performance limits; for instance, a temperature increase in the cell cannot occur stepwise.

## 5 Fuel Cells and DC/DC Converters

Having shown with theorem 4.1 that the electrochemistry in fuel cells poses no inherent limitation to stepping the power output to any design value, we can now look at how this power output may be managed in order to be consistent with an application's requirements. One way is connecting the fuel-cell stack to a DC/DC converter.

A DC/DC converter has the objective of transforming the power from the fuel cell in an appropriate form. According to Luo and Ye [18], there are over 500 different topologies of converters. The most simple are the *boost* converter, that increases voltage from input to output, and the *buck* converter, that decreases it; other types are the *buck-boost* and the *Cuk* converters.

The buck-boost converter is chosen for this paper. The reasons are that it can convert power in a wide range of voltages, both above and below the cell stack's: the buck or the boost converters alone, instead, could only respectively reduce or increase the input voltage. The buck-boost converter is also simpler than the *Cuk* converter, having only two states instead of four.

In a real application, a more complex, four-quadrant converter would probably be preferred. Such a converter would be able to deliver power from the fuel cell to the motor, and to implement regenerative braking by transferring power from the motor to a battery or a capacitor; it would also be able to invert the sign of voltage, to drive and brake the vehicle in reverse. In this study, only the case of a first-quadrant converter will be considered, for sake of simplicity.

### 5.1 Fuel Cells coupled with Converters

In buck-boost converters, we usually have a discontinuous current passing through the input, in our case a fuel cell stack. Since the switching frequency will in most cases be much faster than the transients in the cells, it is common to work with averaged units [19].

Of particular interest is the case of a current stepping between a certain value and zero at regular intervals. Defining  $D$  to be the fraction of time during which a current  $I$  passes through the cell, we find that the reaction current (the one corresponding to the consumption of reactants) is  $I_r = I D$  when averaged over

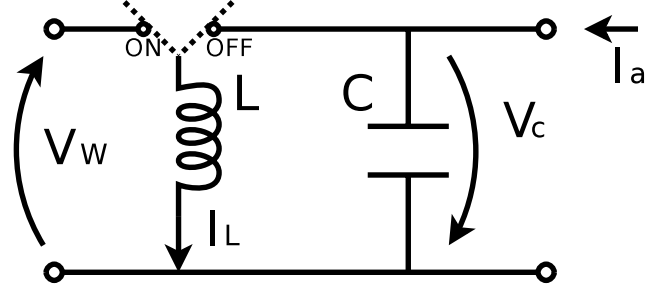


Fig. 8. A basic representation of a buck-boost converter;  $V_W$  is the input voltage.

a sufficiently long time<sup>5</sup>. If the switching frequency is substantially faster than the electrochemical dynamics, we may assume the overvoltage to be constant:  $\eta \approx \eta(iD)$ . However, the cell voltage loss caused by the linear resistance has no transient associated, and will depend directly on the current, no matter it is applied only a fraction of the time. Therefore, calling  $V_W$ , or *working voltage*, the voltage obtained by a fuel cell under a rapidly switching current that has value  $I$  for a fraction  $D$  of the time, we obtain:

$$V_W = E - \eta(iD) - RI \quad (7)$$

This voltage is the actual input voltage that the DC/DC converter will work with.

## 5.2 Buck-Boost Converters

A buck-boost converter is sketched in figure 8. The voltage source is connected in parallel, through a switch, to an inductor. When the switch is on, the inductor accumulates power by storing energy in its magnetic field.

The inductor current varies continuously, as it is a state. When the switch is off, the current is therefore forced into the capacitor that the inductor is now in parallel with, moving the energy stored in the inductor's magnetic field into the capacitor's electric field.

Independently from the switch's state, the capacitor is continuously exchanging power with an external load.

In this layout, we assume that the cell stack's voltage  $V_W$  and the external load's current  $I_a$  are measurable at all times.

Since we know from theorem 4.1 that fuel cells can immediately deliver their

<sup>5</sup> Here we are neglecting the effect of the crossover current for ease of notation.

maximum power, the DC/DC converter parameters will be the main limit to our performance. Lower values for the capacitance and the inductance will increase the transient's speed and accelerate the overall response, but will require faster switching. In this paper we will use the values previously used in a boost converter designed in Caux et al. [13], namely  $L = 0.94$  mH and  $C = 3.2$  mF.

The equations describing this system are, when the fuel-cell stack is connected to the inductor (the ON position in figure 8):

$$L \frac{dI_L}{dt} = V_W \quad (8)$$

$$C \frac{dV_C}{dt} = -I_a \quad (9)$$

$V_W$  and  $I_a$  are considered to be external entities with respect to the converter, and are assumed to maintain a positive sign. The trajectories described by these equations are straight lines, since  $I_a$  and  $V_W$  are assumed not to depend directly on  $I_L$  or  $V_C$ .<sup>6</sup>

When the switch is positioned so that the inductor is connected to the capacitor (the OFF position in figure 8), the equations are instead:

$$L \frac{dI_L}{dt} = -V_C \quad (10)$$

$$C \frac{dV_C}{dt} = I_L - I_a \quad (11)$$

The trajectories described by these equations are a series of ellipses, centred at the point  $(0, I_a)$ , whose parametric equation can be given as:

$$\frac{1}{2}L(I_L - I_a)^2 + \frac{1}{2}C V_C^2 = k \quad k \in \mathbb{R}_0^+ \quad (12)$$

It would be tempting to define these curves as representatives of the amount of energy physically stored in the converter, but the first term in equation 12 is not the energy stored in the inductor's magnetic field. The value of  $k$ , however, can indeed be mathematically interpreted as representative of the system's energy.

---

<sup>6</sup> In reality,  $V_W$  depends on  $I_L$ , as  $V_W = E - \eta - R I_L$ . However, such an assumption would require a cell-specific parameter,  $R$ , to be provided. It will be assumed that  $R$  is small enough to justify an assumption of positive  $V_W$  in the area of interest.



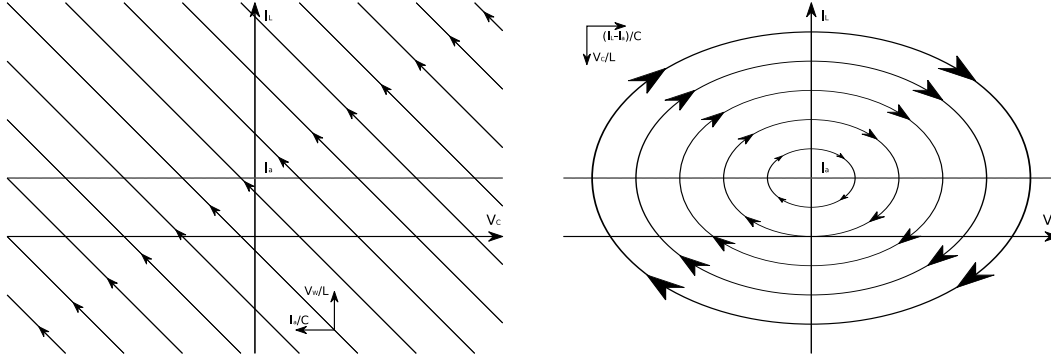


Fig. 9. The trajectories of the state variables in a buck-boost converter in the  $V_C$ - $I_L$  plane. On the left-hand side, energy is collected from the input by the inductor. On the right-hand side, no energy is drawn from the source, and the energy stored in the inductor is exchanged with the capacitor. The capacitor delivers power to the output in both configurations. In a real system, the trajectories in the right-hand sides would be spirals, because of losses in the switches.

The trajectories corresponding to these equations are shown in figure 9.

### 5.3 Control of DC/DC converters

The most common techniques to control a converter are pulse-width modulation [20] and sliding-mode control [21]. In pulse-width modulation, a *duty ratio*  $D$ , representing the fraction of time the switch is in the ON position, is varied between 0 and 1. In sliding-mode control, instead, the switch is set to ON or OFF state depending on a set of logic rules, which are recalculated at very short intervals. Another possible technique is model-predictive control, as suggested by Geyer et al. [22]; since the time required for online optimisation largely exceeds the requirements, the authors suggested using a state-feedback piecewise affine controller [23]. Application of  $\mathcal{H}_\infty$  controllers has also been studied [24].

This paper will adopt an approach similar to sliding-mode control by defining some *switching rules*. Instead of the usual constant sliding surfaces as described by Spiazzi and Mattavelli [21], a series of variable surfaces were devised to take advantage of the shape of trajectories of the system in the  $V_C$ - $I_L$  plane. This is helpful as their shape can change considerably depending on external disturbances (such as  $I_a$  and  $V_W$ ), which represent the effect of having a variable voltage source and an unknown load. This is strictly speaking not sliding-mode control, as no one of the defined surfaces will actually be a sliding mode. The rules, however, do make sure that the desired output is attained.

## 5.4 Control Rules

Control of the converter will be understood having the following objective: *to control the output voltage  $V_C$  so that it is close to reference  $V_{ref}$ , in spite of external disturbances  $I_a$  and  $V_W$ , by manipulating the switch in the buck-boost controller.* In other words, we will try to maintain a certain value of  $V_C$  by properly switching the system between its two substructures (as shown in figures 8 and 9). The rules are formulated as follows:

**Energy level** If the value of  $k$  in equation 12 is not sufficiently high, the elliptical trajectories of the OFF mode will not be able to reach  $V_{ref}$ . Therefore, the only possibility left is to switch to the linear trajectories of the ON mode until a sufficiently high energy level is reached.

The *sufficiently high* energy level is however not the one corresponding to an ellipse that has its extreme point in  $V_{ref}$ . If it were so, it would not be possible to maintain the operating point at that value by switching to the ON mode: the ON mode, which in general has a non-zero component along the  $V_C$  axis, would cause the system to reach a lower energy level, at which it should maintain the ON state until reaching again a high enough energy level. An hysteresis cycle would then result, which would be an unsatisfactory performance.

The correct energy level is then the one corresponding to the ellipse that, at the reference voltage  $V_{ref}$ , is *tangent* to the lines of the ON mode. The unavoidable imprecision in parameter estimation and measurement will cause some oscillation, however.

The mathematical description of the rule is:

$$\frac{1}{2} C V_C^2 + \frac{1}{2} L (I_L - I_a)^2 < \frac{1}{2} C V_{ref}^2 + \frac{1}{2} L \left( \frac{V_{ref} I_a}{V_W} \right)^2 \Rightarrow \text{ON} \quad (13)$$

**High-voltage switch** At voltages higher than  $V_{ref}$ , the surface at which one moves from one substructure to the other is given by the tangent line departing from the ellipse described above, at voltage  $V_{ref}$ . Since this line is by construction parallel to the lines of the ON mode, once the operating points, moving along the OFF-mode ellipses, crosses this line, it is not possible for it to return back. This is important because there is no guarantee that the component of the ON-mode derivatives along a given line are larger than the OFF-mode's, because the former are disturbances that we do not directly control.

The mathematical description of the rule is:

$$V_C > V_{ref} \quad \wedge \quad I_L - I_a < \frac{V_{ref} I_a}{V_W} - \frac{C V_W}{L I_a} (V_C - V_{ref}) \Rightarrow \text{ON} \quad (14)$$

**Low-voltage switch** It is not unlikely that, during transients, voltage  $V_C$  will reach negative values. In fact, it is quite a common phenomenon, albeit

lasting only for a short time. A reasonable control objective is to minimise the inverse response during such a transient. Therefore, if during a transient  $V_C$  is less than zero, and the energy level is sufficient as defined above, the switch from **ON** mode to **OFF** mode should be at the point where the **ON** lines are tangent to an ellipse, which is the lowest-energy point they will reach.

The mathematical description of the rule is:

$$V_C < 0 \quad \wedge \quad I_L - I_a < \frac{V_C I_a}{V_W} \Rightarrow \text{ON} \quad (15)$$

**No negative currents** An additional rule may be easily implemented if we desired to avoid negative values of current  $I_L$ , but the short duration of transients should not pose a threat of reverse electrolysis<sup>7</sup>. However, if that were the case, one could simply implement:

$$I_L < 0 \Rightarrow \text{ON} \quad (16)$$

**Combining the rules** The first three rules (not the rule against negative current) are graphically plotted in figure 10. If no rule should match, the default state of the switch will be **OFF**.

### 5.5 Performance of the Switching Rules

Some preliminary conclusions can be drawn by looking carefully at figure 10.

- Steps in  $V_{ref}$  will in general exhibit an inverse response. When increasing, the operating point will have to accumulate energy along the **ON**-mode lines, which will cause an initial reduction of  $V_C$ . When decreasing, the operating point will follow the **OFF**-mode lines until it will reach either their maximum value of voltage, or the switching surface described by rule 14, before decreasing again.
- Steps in  $I_a$  will have a similar effect, but this is intuitive: more current at the output, at the same output voltage, means more power delivered, and the converter will have to gradually adapt to this new regime.
- The set of rules does not permit to specify a negative  $V_{ref}$ . This is intentional, because, with a positive  $I_a$ , power would be drawn from the outer circuit to the fuel cell, causing reverse electrolysis, and likely damaging the fuel cell's catalyst.

A simulated transient is shown in figure 11. It can be noticed how the inverse response is much more significant at high values of  $I_a$ . The transients have

---

<sup>7</sup> Of course this is relevant only for the **ON** mode, when current is actually passing through the fuel-cell stack.

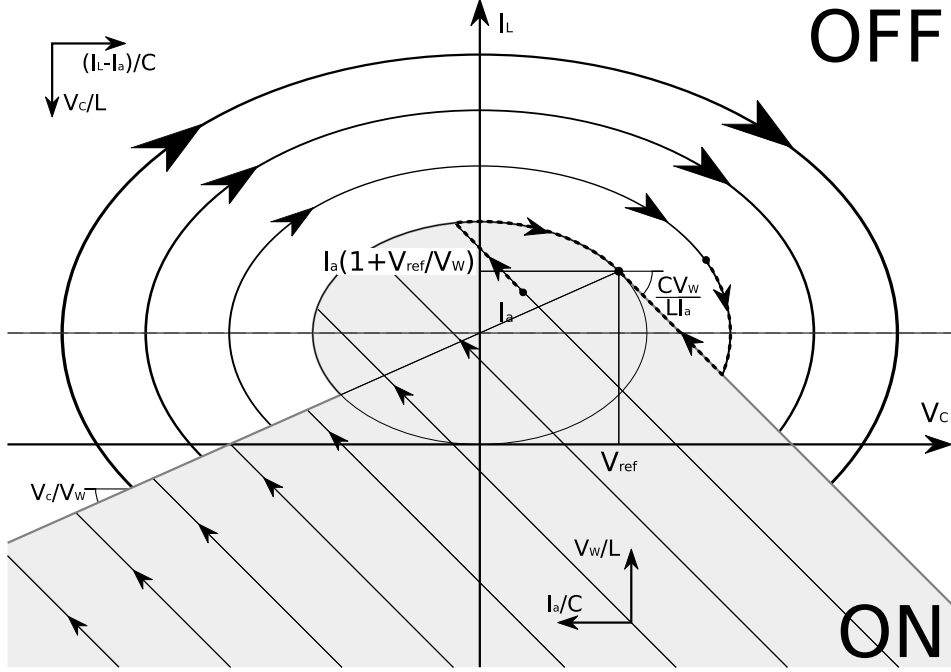


Fig. 10. Graphical representation of the switching rules to control a buck-boost converter. Notice that the inclination of the ON lines (in the greyed-out area), the inclination of the switching lines at high and low voltage, and the size and vertical positioning of the central elliptical part all depend on the values of the reference voltage and the disturbances. Two possible trajectories, from higher and lower values of  $V_C$  to reach  $V_{ref}$ , are sketched.

typically quick settling times, about 5 ms: this is faster than the required 0.2 s (according to Soroush [25]).

The steady-state error that is present in two of the high-voltage regimes shown in figure 11 is due to modelling error. At high values of  $I_a$  and  $V_C$ , the dependence of  $V_W$  on  $I_L$  becomes sufficiently large to prevent convergence. However, the error is small, and, when using this control method in an internal loop of a cascade control layout, the external feedback loop will compensate for this.

### 5.6 Computational efficiency

The simulation times of this controller are relatively long; the transient in figure 11 requires about 50 seconds to calculate on a 2-GHz, 32-bit desktop computer running Simulink. This makes simulation over longer time spans unpractical. The fuel cell's overvoltage, when starting the simulation, needs some time to reach a steady-state value from zero, and this initialisation transient may interfere with the transients we are interested in measuring.

The main reason for such an unsatisfactory computational efficiency is that the

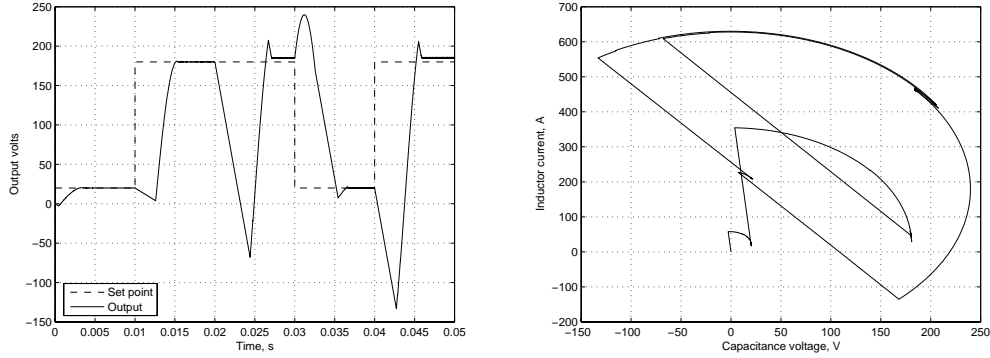


Fig. 11. Simulated transient of a buck-boost converter, controlled with switching rules. The external current is initially 20 A, and is stepped to 180 A after 20 ms. The switching frequency has been set to  $10 \mu\text{s}$ . On the right, a phase-plane plot is presented.

rules are evaluated every  $10 \mu\text{s}$ , and a transient has to be calculated every time the algorithm requires a switch. When the transients settle<sup>8</sup>, the manipulated variable does not attain a constant value, but is continuously switched between ON and OFF.

Using another model that would allow the usage of a continuous manipulated variable and averaged values for other variables would likely improve the simulation performance, even though the control performance might be reduced because of the additional level of abstraction. Pulse-width modulation is another common technique in converter control that might provide these benefits. The option of using pulse-width modulation in this setting is currently being investigated.

## 6 Application to a DC Electric Motor

It has been shown in figure 4 that the shape of the characteristic of the external load has a strong effect on how the transient develops in the fuel cell. It is therefore generally desirable, when designing a controller for a fuel cell, to consider a description of the load as well. In other words, the controller is not for the fuel cell alone, but for the whole system. In this section, an electric motor for a fuel-cell powered car will be considered; for simplicity, a regenerative braking system is not going to be modelled.

<sup>8</sup> In reality, only *macroscopic* transients settle, because the control algorithm is indeed based on rapidly switching between two transients compensating each other.

## 6.1 Electric DC motors

Dual-current motors have for a long time been the only type of electric motor that could be easily controlled. The reason of this preference is due to the simplicity of controlling the main variable in DC motors, the input current, as opposed to the difficulty of controlling the input frequency in alternated-current motors.

Whereas microelectronics has made it practical to control AC motors too, this paper will consider a DC motor as the load to which the fuel cell is connected. So-called “brushless DC motors” are in actuality AC motors with a electronic interface that makes them appear like DC ones to the outside circuit, with the benefit of disposing of the brushes, which are often the main limit to the motor’s lifetime.

Generally speaking, there are two main variables influencing the power output in a DC motor’s mathematical model (figure 12): the armature current and the field-winding current. The armature current,  $I_a$ , is directly proportional to the torque exerted by the motor, divided by the magnetic field  $\Phi_e$ . The voltage generator  $V_m$  in figure 12 represents the counter-electromotive force induced by the rotation of the shaft. Its value is directly proportional to the angular velocity multiplied by the magnetic flux  $\Phi_e$ .

The field-winding current, which usually absorbs just a small fraction of the total power consumption, generates the magnetic field in which the armature current passes; by weakening the field, it is possible to increase velocity at the expense of torque, by modifying the proportionality ratio between armature current and torque [26]. However, for vehicle applications, higher velocity usually means higher torque too, because of wind resistance: in this paper, therefore, a permanent-magnet motor will be considered, or, equivalently, a motor with constant field winding current.

Such a simplified model can be described by the following equations:

$$V_a = R_a I_a + L_a \frac{dI_a}{dt} + V_m \quad (17)$$

$$V_m = k v \quad (18)$$

$$I_a = \frac{F}{k} \quad (19)$$

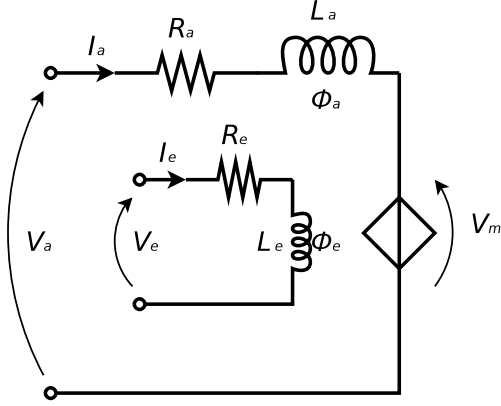


Fig. 12. A typical model of a DC motor [26].

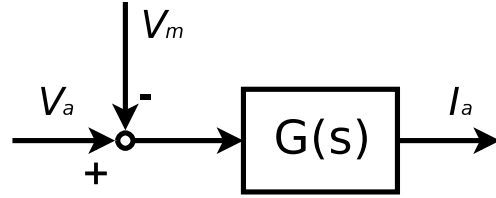


Fig. 13. The process flow diagram of a simple DC motor with constant magnetic flow; its transfer function is expressed by  $G = \frac{1}{L_a s + R_a}$ , as shown in equation 22.

### 6.1.1 Value of $k$

Constant  $k$  is the same in equations 18 and 19, since the electric power input must be equal to the mechanical power output ( $F v = V_m I_a$ ). Constant  $k$  includes the rotation radius as well, so that we may work in terms of force  $F$  applied by the motor to the vehicle and the vehicle's velocity  $v$  instead of the motor's torque  $T$  and angular velocity  $\omega$ . In practice, constant  $k$  can be set with a gearbox [27].

Larminie and Lowry [27] claim that a common parameter for electric-vehicle motors is a maximum nominal armature current of 250 A. Considering that a driving cycle such as the New European Driving cycle, with common values [10], results in a maximum force requirement of about 1250 N, we can use equation 19 to obtain a reasonable value for  $k$ :

$$k = \frac{F}{I_a} \approx 5 \text{ N A}^{-1} \quad (20)$$

### 6.1.2 Control Variables

Rearranging equation 17, we can more easily see that  $I_a$  is a state<sup>9</sup> of the motor.

<sup>9</sup> *State* means here a variable that is a differential state in an ordinary differential equation.

$$L_a \frac{dI_a}{dt} = V_a - R_a I_a - V_m \quad (21)$$

From here, it is easy to transpose this equation in the Laplace domain:

$$I_a = \frac{1}{L_a s + R_a} (V_a - V_m) \quad (22)$$

Typical values of 20 mH for  $L_a$  and 20 m $\Omega$  for  $R_a$  will be used. For more data, refer to Larminie and Lowry [27], Leonhard [26], or Ong [28].

A graphical representation of this system is presented in figure 13. We see clearly that  $I_a$  is the output and  $V_a - V_m$  is the input.

Since  $V_m$  is a direct consequence of vehicle motion, it is not possible to modify it without acting on the vehicle speed; this would be undesirable, because the driver will control manually the velocity by acting on the accelerator pedal (and therefore  $I_a$ ). The counter-electromotive force  $V_m$  will therefore be interpreted as a *disturbance*.

It is however possible to compensate for this disturbance by manipulating the input voltage  $V_a$ . The control problem is therefore to control  $I_a$  by manipulating  $V_a$ , in spite of disturbance  $V_m$ .

We can set voltage  $V_a$  by connecting the motor input to a buck-boost converter's output. The control performance that was indicated in the section on converter control can be now interpreted as *actuator dynamics*. This is an example of *cascade control*: control of  $I_a$  is obtained by controlling  $V_C$ , which is in turn obtained by switching between the buck-boost converter's ON and OFF modes.

## 6.2 Approximation of a buck-boost converter

In order to obtain a controller, it can be useful to approximate the actuator dynamics as a transfer function. Looking at figure 11, we can assume that the actuator dynamics can be approximated by the following transfer function:

$$A(s) = \frac{e^{-\theta s}}{\tau s + 1} \quad (23)$$

Where the delay  $\theta$  is estimated at 4 ms and the time constant  $\tau$  at 1.5 ms. The delay  $\theta$  is assumed to be an *effective* delay, actually representing the inverse



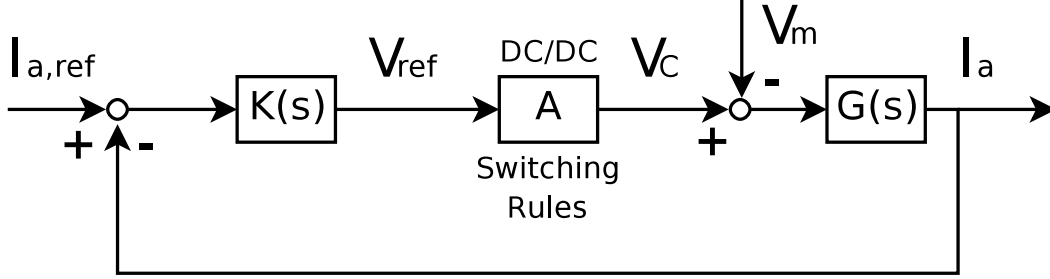


Fig. 14. The control structure of the proposed layout.

response; Skogestad [29] claims that “an inverse response has a deteriorating effect on control similar to that of a time delay”.

### 6.3 PI Controller Synthesis

Having a complete, however approximate description of the system, we can proceed to synthesise a PI controller according to the SIMC rules [29]. The resulting controller is:

$$K(s) = K_c \left( 1 + \frac{1}{\tau_I s} \right) \quad (24)$$

Where we select  $K_c = 3.125$  and  $\tau_I = 32$  ms.

It is now possible to make simulation runs of the whole control system. However, due to the complexity that the model has attained at this point, especially in its rapid switching rules for the DC/DC converter, it is not practical, in terms of computational time, to simulate an entire driving cycle as those issued by various authorities. On a 2-GHz, 32-bit computer, the simulations in figure 15 take about 90 seconds; on the same computer and in equal conditions, the transient with a linear  $A(s)$  is calculated almost instantaneously.

As an indicator of performance, the linear approximation of equation 23 may be used, but it will obviously not give any information about the fuel cell during the simulation run. It is expected that using control methods based on averaged quantities, such as pulse-width modulation, will reduce the requirements to the point where simulations in the range of hours will be reasonably computationally cheap.

Using the current complete model, however, one can simulate some specific transients and observe the control performance.

A brief series of transients is simulated in figure 15. It is assumed a vehicle

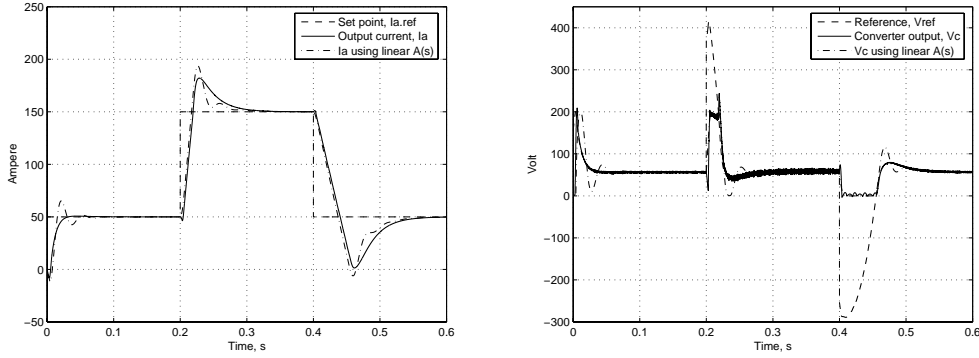


Fig. 15. Simulation of a series of steps in reference for the system in figure 14. On the left, the set point  $I_{a,ref}$  and value of the armature current in the electric motor  $I_a$ . On the right, the PI controller's output  $V_{ref}$  is the reference signal for the DC/DC converter. The switching frequency in the converter is  $100 \mu\text{s}$ . In both plots, the results obtained using the linear approximation for the converter presented in equation 23, instead of the complete nonlinear model, are also shown. The output of the controller has been limited to  $V_{ref} \in [0, 200]$  V.

is moving at  $40 \text{ km/h}^{10}$ , and that a series of steps in the armature current's reference<sup>11</sup> are performed.

The resulting control performance seems to be satisfactory, with rise times of at most 50 ms in all transients; some overshoot is observed, but the transient is settled in all cases after 0.2 s.

#### 6.4 Limitations on controller output

In the simulation, the output of the controller has been limited to  $V_{ref} \in [0, 200]$  V. Therefore, when the controller would require a value outside this interval, the exceeding amount of control action will be ignored. This can, in principle, cause problems related to wind-up; indeed, the transients presented appear to be consistently slower when their manipulated variable has been saturated for a longer time.

While the upper bound on  $V_C$  is somewhat arbitrary, under no condition should it be made possible for the controller to require a negative voltage. This would mean that power is being absorbed in the fuel-cell stack, and reverse electrolysis or other damaging phenomena will rapidly occur. In this configuration, the reduction of  $I_a$  is possible only through the disturbance  $V_m$  (proportional to vehicle velocity) and through resistance  $R_a$ , with a time

<sup>10</sup> The speed is kept constant in the simulation, for simplicity and to make the results comparable.

<sup>11</sup> Steps in the armature current are proportional to steps in torque.

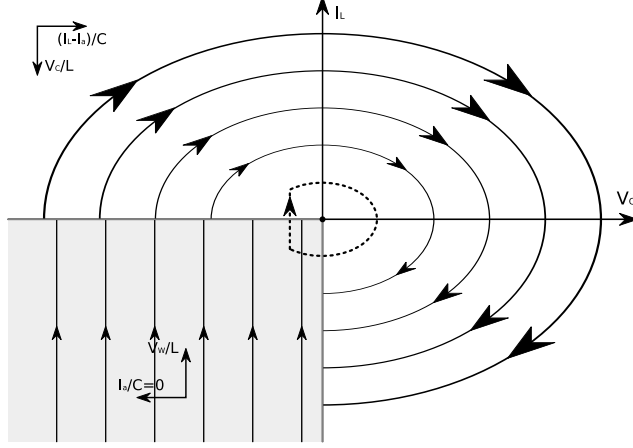


Fig. 16. The approximate trajectory of the operating point when  $V_{ref} = 0$  and  $I_a = 0$ . Higher switching frequencies will shrink the trajectory towards the origin.

constant of about one second. In fact, with the proposed control configuration, the control system may experience significant wind-up problems in a case as trivial as  $I_{a,ref} = 0$ ,  $V_m = 0$ , that is a vehicle standing still. In a real vehicle, this would just translate to some torque in the motor being compensated by braking action.

Another issue is when the converter is required to produce exactly 0 volts, even if  $I_a$  is larger than 0. This happens anytime the PI controller requires a negative voltage. The converter's switching rules degenerate in a special case: output voltage oscillates around the origin in an asymmetrical fashion, sketched in figure 16, resulting in a net average positive value of  $V_C$  and possibly wind-up issues. This is visible in figure 15 at the beginning of the last transient. While the amplitude of such oscillations can be reduced with a higher switching frequency, their average value will always be positive.

To resolve this problem, a new simple rule for the converter will be added:

$$V_{ref} \leq 0 \Rightarrow \text{OFF} \quad (25)$$

It is important to notice that rule 25 takes precedence on all others, since it might be contradicting them. The meaning of this rule is that the fuel-cell stack must be disconnected whenever there is an unachievably low objective. In a real application, the voltage will then gradually decrease to zero because of dissipation in the motor and in the converter switches, or because of storage in a battery or supercapacitor.

The last transient of figure 15 with this new rule is shown in figure 17. There is a clear oscillatory interval where the average value of  $V_C$  is zero. The overall dynamics may be marginally faster, but the most important result is the disconnection of the fuel-cell stack when its power is not needed.

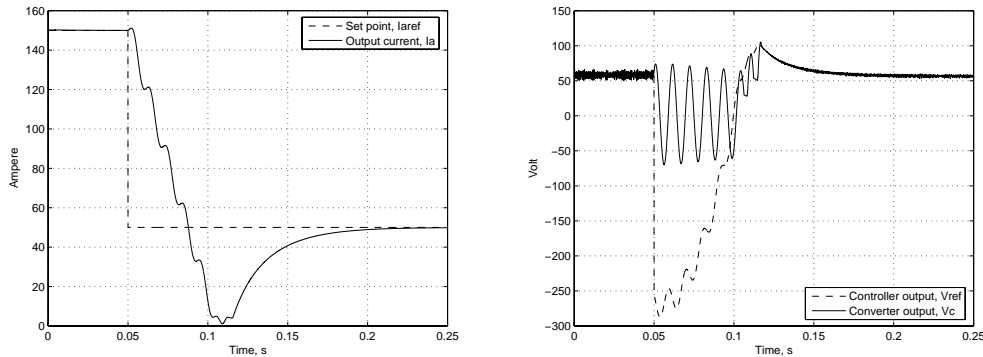


Fig. 17. Recreation of the last transient in figure 15 after the introduction of rule 25.

## 7 Conclusion

This article has first analysed from a theoretical point of view the electrochemical transient of fuel cells, introducing the concept of instantaneous characteristic of a fuel cell and how it influences the shape of transients in the voltage-current density phase plane.

These results have been used to demonstrate that it is always possible to instantaneously step the power output of a fuel cell to its maximum (meant as the maximum at the present temperature, partial pressures, catalyst poisoning etc.) under broad conditions.

A method to control the output voltage of a buck-boost converter connected to a fuel cell was presented. The method is based on switching the converter based on a few simple logical rules. The resulting performance has been deemed satisfactory, with transients settling after about 5 milliseconds. The requirements on computational time for this strategy, however, make it difficult to simulate the control system over longer time spans, such as standard driving cycles; using an averaged-quantity method such as pulse-width modulation is suggested as a means to improve the computational performance.

The resulting control loop has then been inserted in a cascade-control framework (figure 14) to control the armature current in a DC motor by manipulating its input voltage. The results have been in excess of specifications given elsewhere in the literature [25], with rise times of about 50 milliseconds and settling times of less than 0.2 seconds (figure 15).

## Acknowledgements

This work has received financial support from the Norwegian Research Council and Statoil AS.

## References

- [1] J. C. Amphlett, R. F. Mann, B. A. Peppley, P. R. Roberge, A. Rodrigues, A model predicting transient responses of proton exchange membrane fuel cells, *Journal of Power Sources* 61 (1996) 183–188.
- [2] M. Ceraolo, C. Miulli, A. Pozio, Modelling static and dynamic behaviour of proton exchange membrane fuel cells on the basis of electro-chemical description, *Journal of Power Sources* 113 (2003) 131–144.
- [3] P. R. Pathapati, X. Xue, J. Tang, A new dynamic model for predicting transient phenomena in a PEM fuel cell system, *Renewable energy* 30 (2005) 1–22.
- [4] H. Lorenz, K.-E. Noreikat, T. Klaiber, W. Fleck, J. Sonntag, G. Hornburg, A. Gaulhofer, Method and device for vehicle fuel cell dynamic power control, US patent 5 646 852, assigned to Daimler-Benz Aktiengesellschaft (July 1997).
- [5] W. E. Mufford, D. G. Strasky, Power control system for a fuel cell powered vehicle, US patent 5 771 476, assigned to DBB Fuel Cell Engines GmbH (June 1998).
- [6] J. T. Pukrushpan, Modeling and control of fuel cell systems and fuel processors, Ph.D. thesis, Department of Mechanical Engineering, University of Michigan, Ann Arbor, Michigan, USA (2003).
- [7] L. Guzzella, Control oriented modelling of fuel-cell based vehicles, in: NSF workshop on the integration of modeling and control for automotive systems, 1999.
- [8] H. Weydahl, S. Møller-Holst, G. Hagen, Transient response of a proton exchange membrane fuel cell, in: Joint International Meeting of The Electrochemical Society, 2004.
- [9] F. Zenith, F. Seland, O. E. Kongstein, B. Børresen, R. Tunold, S. Skogestad, Control-oriented modelling and experimental study of the transient response of a high-temperature polymer fuel cell, *Journal of Power Sources* (submitted 2006).
- [10] R. L. Johansen, Fuel cells in vehicles, Master’s thesis, Norwegian University of Science and Technology (2003).
- [11] J. Golbert, D. R. Lewin, Model-based control of fuel cells: (1) regulatory control, *Journal of Power Sources* 135 (2004) 135–151.

- [12] J. Benziger, oral comment at the annual meeting of the American Institute of Chemical Engineers in Austin (2004).
- [13] S. Caux, J. Lachaize, M. Fadel, P. Shott, L. Nicod, Modelling and control of a fuel cell system and storage elements in transport applications, *Journal of Process Control* 15 (2005) 481–491.
- [14] A. Parthasarathy, B. Davé, S. Srinivasan, A. J. Appleby, C. R. Martin, The platinum microelectrode/Nafion interface: An electrochemical impedance spectroscopic analysis of oxygen reduction kinetics and Nafion characteristics, *Journal of the Electrochemical Society* 139 (6) (1992) 1634–1641.
- [15] C. H. Hamann, A. Hamnet, W. Vielstich, *Electrochemistry*, Wiley-VCH, 1998.
- [16] J. Larminie, A. Dicks, *Fuel Cell Systems Explained*, 1st Edition, Wiley, 1999.
- [17] N. Mohan, T. M. Undeland, W. P. Robbins, *Power Electronics: Converters, Applications and Design*, 2nd Edition, John Wiley & Sons, Inc., 1995.
- [18] F. L. Luo, H. Ye, *Advanced DC/DC Converters*, CRC press, Boca Raton, Florida, USA, 2004.
- [19] J. P. Agrawal, *Power Electronic Systems — Theory and Design*, Prentice Hall, 2001.
- [20] M. Giesselmann, H. Salehfar, H. A. Toliyat, T. U. Rahman, *The Power Electronics Handbook*, Industrial electronics, CRC press, 2001, Ch. 7 - Modulation Strategies.
- [21] G. Spiazzi, P. Mattavelli, *The Power Electronics Handbook*, Industrial electronics, CRC press, 2001, Ch. 8 - Sliding-Mode Control of Switched-Mode Power Supplies.
- [22] T. Geyer, G. Papafotiou, M. Morari, On the optimal control of switch-mode DC-DC converters, *Hybrid Systems: Computation and Control* 2993 (2004) 342–356.
- [23] M. Morari, Beyond process control, in: *Proceedings of the 13th Nordic Process Control Workshop*, Lyngby, Denmark, 2006.
- [24] R. Naim, G. Weiss, S. Ben-Yaakov,  $H^\infty$  control applied to boost power converters, *Transactions on Power Electronics* 12 (4) (1997) 677–683.
- [25] M. Soroush, Y. A. Elabd, Process systems engineering challenges in fuel cell technology for automobiles, in: *AICHE Annual Meeting*, 2004.
- [26] W. Leonhard, *Control of Electrical Drives*, 2nd Edition, Springer, 2001.
- [27] J. Larminie, J. Lowry, *Electric Vehicle Technology Explained*, Wiley, 2003.
- [28] C.-M. Ong, *Dynamic Simulation of Electric Machinery*, Prentice Hall, 1998.
- [29] S. Skogestad, Simple analytic rules for model reduction and PID controller tuning, *Journal of Process Control* 13 (2003) 291–309.